

Analyzing the Effect of Loadability in the Presence of TCSC & SVC

M. LakshmiKantha Reddy¹, V. C. Veera Reddy²,

Research Scholar, Department of Electrical Engineering, SV University, Tirupathi, India¹

Professor and Head (Rtd), Department of Electrical Engineering, SV University, Tirupathi, India²

ABSTRACT: The loadability enhancement problem with loadability objective is solved in the presence of TCSC and SVC while satisfying system equality and in-equality constraints. It is necessary to solve the optimal power flow in the presence of series and shunt flexible AC transmission system controllers such as thyristor controlled series capacitor and static VAR compensators. The optimal location of these controllers is identified so as to maximize the system security. The optimal parameters of this controller and system are identified using the developed gravitational search algorithm. The effectiveness of the proposed methodology with TCSC and SVC is tested on standard IEEE-30 bus test system with supporting numerical and as well as graphical results.

KEYWORDS: Optimal power flow, Gravitational search algorithm, Loadability, TCSC, SVC, Optimal location

I. INTRODUCTION

To maintain continuity in supply in meeting the continuous increase in load on a given system, it is necessary to operate the power system at its maximum limits i.e. increasing the utilization of the existing transmission network to meet the load. For this, the system loadability must be identified for the secured operation of the power system. From this, the amount of load that we can increase on a given system can be identified. Because of this, the preventive and corrective suggestions can be sent to the operators at the generating as well as transmission systems. Because of increase of the load on a system, the power flow in transmission line is increased. Sometimes, there is a chance of overloading the transmission lines. To avoid such uncontrolled conditions, the loading margin on a system must be identified to avoid the system collapse conditions.

A detailed methodology to identify and optimal number and its optimal location to install multiple series devices were presented in [1, 2]. The proposed methodology uses the differential evolution algorithm to identify optimal parameter settings to enhance the system loadability subjected to various system constraints. The device control parameters are adjusted, so that the device installation cost was minimized without any violation of system thermal and voltage limits. In this paper, the convergence characteristic of the proposed methodology is compared with the existing genetic algorithm.

The loadability of power system is enhanced more by placing shunt devices in an optimal location [3, 4, 5, 6, 7, 8]. In this, the optimal location is identified based on worst case reactive power margin as an index. It is also identified that, the effect of increase of active power demand on a given system. The FACTS controller is used to enhance the voltage stability under most critical conditions of power system. The device location is identified using multi-objective optimization problem by considering device installation cost, highest load voltages, maximum worst case reactive power margin and minimized real power losses.

There are various optimization algorithms in the literature [9, 10, 11] concentrates in finding a methodology to increase the reactive loading margin to increase the loadability on a given system based on non-linear and non-convex optimization techniques. The results obtained through this can be implemented directly in real time power system operation, planning and management. But, because of this methodology larger systems can't be handled in the presence of some of the pertinent constraints or some of the smaller disturbances.

International Journal of Innovative Research in Science, Engineering and Technology

(An ISO 3297: 2007 Certified Organization)

Website: www.ijirset.com

Vol. 6, Issue 4, April 2017

In this chapter, the OPF problem is solved with transmission losses as an objective is solved. The effect of TCSC and SVC in minimizing the objective function is analyzed. Numerical analysis is carried out on standard IEEE-30 bus system to demonstrate the performance of the TCSC and SVC.

II. OPERATING PRINCIPLE OF TCSC

TCSC is one of the series compensator; it can capable to control power flow in line, damping power oscillations [14]. Basic simple TCSC model is shown in Fig.1. TCSC is formed by connecting the capacitor in series with the transmission line and thyristor-controlled reactor (TCR) in parallel with capacitor.

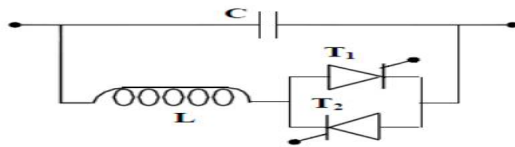


Fig.1 Model of TCSC

2.1 Power Injection Model of TCSC

The Fig.2 shows a π model of transmission line with TCSC connected between bus-k and bus-m [6]. Under the steady state condition, the TCSC can be represented as a static reactance $-jX_C$. In the power flow equations the controllable reactance X_C is directly used as the control variable.

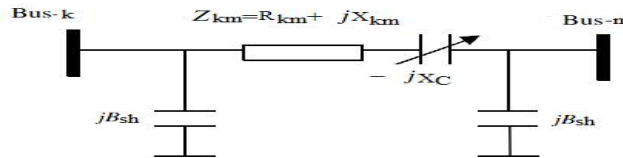


Fig.2 Transmission line with TCSC

The line data will be modified by placing TCSC in series with line. A new line reactance is given as follows

$$X_{km}^{new} = X_{km} - X_C \tag{1}$$

Therefore new line admittance between buses k and m can be derived as follows

$$Y'_{km} = \frac{1}{Z'_{km}} = \frac{1}{R_{km} + j(X_{km} - X_C)} \tag{2} \quad Y'_{km} = G'_{km} + jB'_{km} = \frac{R_{km} - j(X_{km} - X_C)}{R_{km}^2 + (X_{km} - X_C)^2}$$

$$G'_{km} = \frac{R_{km}}{R_{km}^2 + (X_{km} - X_C)^2} \tag{3} \quad B'_{km} = -\frac{(X_{km} - X_C)}{R_{km}^2 + (X_{km} - X_C)^2} \tag{4}$$

(5)

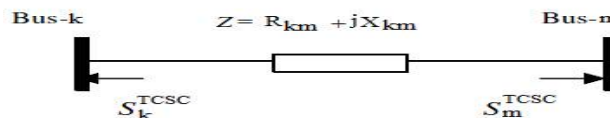


Fig.3 Power injection model of TCSC

Due to TCSC, the change in line flow can be represented as a line without TCSC plus with power injected at the sending and receiving ends of the line with device as shown in Fig.3. The active and reactive power injections at bus-k and bus-m can be written as

$$P_k^{TCSC} = P_{km} - P_{km}^{TCSC} = V_k^2 \Delta G_{km} - V_k V_m [\Delta G_{km} \cos(\delta_{km}) + \Delta B_{km} \sin(\delta_{km})] \tag{6}$$

$$P_m^{TCSC} = P_{mk} - P_{mk}^{TCSC} = V_m^2 \Delta G_{km} - V_k V_m [\Delta G_{km} \cos(\delta_{km}) - \Delta B_{km} \sin(\delta_{km})] \tag{7}$$

$$Q_k^{TCSC} = Q_{km} - Q_{km}^{TCSC} = -V_k^2 \Delta B_{km} - V_k V_m [\Delta G_{km} \sin(\delta_{km}) - \Delta B_{km} \cos(\delta_{km})] \tag{8}$$

International Journal of Innovative Research in Science, Engineering and Technology

(An ISO 3297: 2007 Certified Organization)

Website: www.ijirset.com

Vol. 6, Issue 4, April 2017

$$Q_m^{TCSC} = Q_{mk} - Q_{mk}^{TCSC} = -V_m^2 \Delta B_{km} + V_k V_m [\Delta G_{km} \sin(\delta_{km}) + \Delta B_{km} \cos(\delta_{km})] \quad (9)$$

Where,

$$\Delta G_{km} = \frac{X_C R_{km} (X_C - 2X_{km})}{(R_{km}^2 + X_{km}^2)(R_{km}^2 + (X_{km} - X_C)^2)} \quad (10) \quad \Delta B_{km} = \frac{-X_C (R_{km}^2 + X_C X_{km} - X_{km}^2)}{(R_{km}^2 + X_{km}^2)(R_{km}^2 + (X_{km} - X_C)^2)}$$

(11)

TCSC device is modeled with power injection model so far by using the TCSC control variable. It is possible to calculate the complex power injected S_k^{TCSC} and S_m^{TCSC} at bus-k and bus-m respectively.

$$S_k^{TCSC} = P_k^{TCSC} + jQ_k^{TCSC} \quad (12) \quad S_m^{TCSC} = P_m^{TCSC} + jQ_m^{TCSC}$$

(13)

Then new power flow equations can be expressed by the following relationship

$$\begin{bmatrix} \Delta P \\ \Delta Q \end{bmatrix} = \begin{bmatrix} H_{new} & N_{new} \\ J_{new} & L_{new} \end{bmatrix} \begin{bmatrix} \Delta \delta \\ \frac{\Delta V}{V} \end{bmatrix}$$

(14)

here new mismatch vectors are

$$\Delta P_i = P_k^{spec} + P_k^{TCSC} - P_k^{calc} \quad (15) \quad \Delta Q_i = Q_k^{spec} + Q_k^{TCSC} - Q_k^{calc}$$

(16)

Where, P_k^{spec} , Q_k^{spec} are the classical specified real and reactive powers, P_k^{TCSC} , Q_k^{TCSC} are the power injection associated to TCSC devices, P_k^{calc} , Q_k^{calc} are computed using the power flow equations. Now modified Jacobian matrix due to power injections of TCSC

$$H_{new} = H + \frac{\partial P^{TCSC}}{\partial \delta} ; \quad N_{new} = N + \frac{\partial P^{TCSC}}{\partial V} V \quad (17)$$

$$J_{new} = J + \frac{\partial Q^{TCSC}}{\partial \delta} ; \quad L_{new} = L + \frac{\partial Q^{TCSC}}{\partial V} V \quad (18)$$

H, M, N and L are the classic sub-Jacobians.

2.2 Device limits

The following minimum and maximum limits are considered for TCSC reactance.

$$-0.8X_{line} \leq X_{TCSC} \leq 0.2X_{line} \quad p.u.$$

III. OPTIMAL LOCATION FOR TCSC

The power flows of highest severe contingency are considered as base case. From these flows, the branch with least power flow can be considered as the best location for the TCSC device. Because the transmission line has inductive reactance where as the TCSC is a series controlled device which can provide a capacitive reactance so that the total reactance of the branch which leads to the increase of loadability of the line where the device was located. The objective is, to increase the power transfer capability of the transmission line. The power transfer capability of the transmission line depends on the line reactance as well as bus voltages. Hence the loadability of the line can be increased either by reducing line reactance or increasing voltage profile. In order to reduce the reactance of the transmission line TCSC can be used. The voltage profile can be improved by injecting the reactive power at a particular bus where the voltage is minimum. The optimal location of the device is that where it gives maximum benefit for optimal size of FACTS devices placed at selected location.

3.1 Contingency analysis

Usually, outage of one of the transmission lines can be considered as the contingency condition. This happens due to many reasons; it may be because of maintenance of the transmission lines, environmental conditions, etc. Because of this situation, the transmission lines get overloaded. This contingency analysis analyzes the system security

International Journal of Innovative Research in Science, Engineering and Technology

(An ISO 3297: 2007 Certified Organization)

Website: www.ijirset.com

Vol. 6, Issue 4, April 2017

and gives future directions for the proper planning and designing. Because of this analysis, the preventive and corrective measures under contingency conditions can be predicted. Usually, the contingency condition may be due to a transmission line or a generator failure or a transformer failure. Out of which, transmission line failure plays an important role to assess the power system security.

3.2 Performance Index and Ranking

It is not required to consider each and every line outage to assess power system security. Because, for a particular line outage, there are few lines and buses do not have line flow and voltage variations beyond the limits. If there are any line overloads and bus voltage variations then the outage line is considered as critical line. The critical lines or credible contingencies are identified by contingency analysis and only these critical lines need to be taken to assess the power system security. A parameter which is known as performance index used for security analysis [15]. It indicates how much a particular outage might affect the security of power system. In general the performance index (PI) or severity index (SI) is defined as

$$\text{Severity index} = \sum_{l=1}^{N_{line}} \left(\frac{S_l}{S_l^{max}} \right)^{2m} \quad (19)$$

Where, S_l, S_l^{max} are the MVA flow in line 'l' and MVA rating of the line 'l' respectively. 'm' is an integer exponent taken as 0.5.

The line flows are obtained by using power flow solution method. In Eqn. (19), the performance index is defined only based on over loaded lines.

IV. STATIC VAR COMPENSATOR

The IEEE definition of the SVC is as follows: "A shunt connected static VAR generator or absorber whose output is adjusted to exchange capacitive or inductive current so as to maintain or control specific parameters of the electrical power system (typically bus voltage)."

SVCs are used in a given power systems to enhance the voltage levels so that system stability has been improved.

4.1 Power injection model of SVC

In practice the SVC can be seen as an adjustable reactance with either firing-angle limits or reactance limits [16]. The equivalent circuit shown in Fig.3.4 is used to derive the SVC nonlinear power equations and the linearized equations required by Newton's method. With reference to Fig.4, the current drawn by the SVC is

$$I_{SVC} = jB_{SVC}V_i \quad (20)$$

and the reactive power drawn by the SVC, which is also the reactive power injected at bus-i, is

$$Q_{SVC} = Q_i = -V_i^2 B_{SVC} \quad (21)$$

It is a bank of three-phase static capacitors and/or inductors. Under heavy loading conditions, when positive VAR is needed, capacitor banks are needed, when negative VAR is needed, inductor banks are used. In this thesis SVC is modeled as an ideal reactive power injection at bus-i shown in Fig.4.

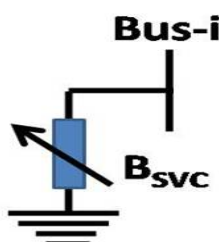


Fig.4. Power injection model of SVC

International Journal of Innovative Research in Science, Engineering and Technology

(An ISO 3297: 2007 Certified Organization)

Website: www.ijirset.com

Vol. 6, Issue 4, April 2017

4.2 Installation cost of SVC

The Installation Cost (IC) [16] of SVC can be expressed as

$$IC_{SVC} = \frac{C_{SVC} \times S_{SVC} \times 1000}{n \times 8760} \quad ; \quad \$/h \quad (22)$$

Here, Cost of Installation of SVC is

$$C_{SVC} = 0.0003S_{SVC}^2 - 0.3051S_{SVC} + 127.38 \quad ; \quad \$/kVAr$$

Operating range of SVC (S_{SVC}) in MVar is $S_{SVC} = |Q_{SVC}|$

Where, Q_{SVC} is the reactive power injected by SVC.

4.3 Device limits

The following limits are considered for SVC

$$-100 \text{ MVar} \leq Q_{SVC} \leq 100 \text{ MVar}$$

4.4 Selection of optimal location for SVC

The SVC should be placed in an optimal location to enhance the system stability.

4.4.1 Voltage Stability Index

The voltage stability index or L -index gives literally consistent results for voltage collapse prediction compared to other methods [17]. The L -indices are computed for all the load buses. The L -index gives a scalar integer to each load bus. The maximum of the L -indices gives the proximity of the system to voltage collapse. The benefit of this method is the simplicity of the numerical calculation and clarity of the results. For the given operating conditions, the voltage stability index is computed using load flow results and is given by

$$L_j = \left| 1 - \sum_{i=1}^{NG} F_{ij} \frac{V_i}{V_j} \right| \quad (23)$$

Where, $j = NG + 1, \dots, NB$, V_i and V_j are the complex voltages of i^{th} and j^{th} bus respectively, F_{ji} are the complex elements of the matrix $[F_{LG}]$.

The matrix $[F_{LG}]$ is obtained from the bus admittance matrix $[Y_{bus}]$.

If the L -index values for load buses are close to zero, indicates the system has maximum stability margin. If it is close to one, indicates the system is close to voltage collapse.

The following procedure is used to identify suitable SVC location and incorporation procedure.

Step1: Perform Newton Raphson load flow on a given system.

Step2: Obtain the system bus voltage magnitude values.

Step3: Calculate the Voltage Stability Index (VSI) at load buses.

Step4: Place the SVC at the bus, where the VSI value is high when compared to other buses.

Step5: In this location, with SVC, the VSI value has been enhanced.

V. OPF PROBLEM FORMULATION

The aim of optimal power flow solution is, to optimize the selective objective function through proper adjustment of control variables by satisfying various constraints. The OPF problem can be represented as follows:

$$\text{Min } [A_m(x, u)] \quad (24)$$

Subjected to $g(x, u) = 0$ and $h_{min} \leq h(x, u) \leq h_{max}$

Where, $A_m(x, u)$ is the function which is to be minimized

$g(x, u)$, $h(x, u)$ represents equality and inequality constraints

'x' and 'u' are dependent and independent variables

International Journal of Innovative Research in Science, Engineering and Technology

(An ISO 3297: 2007 Certified Organization)

Website: www.ijirset.com

Vol. 6, Issue 4, April 2017

Optimal power flow solution gives an optimal control variable leads to the minimum generation fuel cost, emission and total power loss etc. subjected to all the various equality and inequality constraints. Here the vector 'x' consists of slack bus real power output (P_{G_1}), generator VAR output (Q_G), load bus voltage magnitude (V_L), line flow limits (S_l)

Thus 'x' can be written as,

$$x^T = [P_{G_1}, V_{L_1}, \dots, V_{L_{NL}}, Q_{G_1}, \dots, Q_{G_{NG}}, S_{l_1}, \dots, S_{l_{nl}}] \quad (25)$$

Where, NL=Number of load buses, NG=Number of generator buses, nl=Number of lines, u= is the independent variable vector such as continuous and discrete variables consists of

- (i) Generator active output 'P_G' at all generators without slack bus
- (ii) Generator voltages V_G
- (iii) Tap settings of transformer 'T'
- (iv) Shunt VAR compensation(or) reactive power injections Q_C

Here PG, VG are continuous variables and T and QC are the discrete variables. Hence 'u' can be expressed as

$$u^T = [P_{G_2}, \dots, P_{G_{NG}}, V_{G_1}, \dots, V_{G_{NG}}, Q_{C_1}, \dots, Q_{C_{nc}}, T_1, \dots, T_{NT}] \quad (26)$$

'NT' and 'nc' re number of tap controlling transformers and shunt compensators.

5.1 Loadability index objective function

The real and reactive power balance equations at ith bus can be expressed as

$$\sum_{\forall i} P_{G_i} - \sum_{\forall i} (1 + \lambda) P_{D_j} - \sum_{\forall k} P_{ik} = 0 \quad (28)$$

$$\sum_{\forall i} Q_{G_i} - \sum_{\forall i} (1 + \lambda) Q_{D_j} - \sum_{\forall k} Q_{ik} = 0 \quad (29)$$

Where, P_{G_i} and Q_{G_i} are the real and reactive power generations at ith, P_{D_j} and Q_{D_j} are the real and reactive power loads at jth bus under base case condition ($\lambda = 0$) P_{lk} and Q_{lk} are the real and reactive power losses at kth line.

$$A_5 = \text{Loadability} = \max(\lambda) \quad (30)$$

The maximum additional loading of the system, $\lambda \times \sum P_{D_j}$ can be obtained.

5.2 Constraints

Constraints made in this OPF problem are usually two types. They are equality constraints and inequality constraints.

5.2.1 Equality constraints

These constraints mentioned in Eqn. (29) are usually load flow equations described as

$$P_{g,k} - P_{d,k} - \sum_{m=1}^{N_{bus}} |V_k| |V_m| |Y_{km}| \cos(\theta_{km} - \delta_k + \delta_m) = 0 \quad (31)$$

$$Q_{G,k} - Q_{d,k} - \sum_{m=1}^{N_{bus}} |V_k| |V_m| |Y_{km}| \sin(\theta_{km} - \delta_k + \delta_m) = 0 \quad (32)$$

where $P_{G,k}$, $Q_{G,k}$ are the active and reactive power generation at the k^{th} bus, P_{dk} , Q_{dk} are the active and reactive power demands at the k^{th} bus, $|V_k|$, $|V_m|$ are the voltage magnitudes at the k^{th} and m^{th} buses, δ_k , δ_m are the

International Journal of Innovative Research in Science, Engineering and Technology

(An ISO 3297: 2007 Certified Organization)

Website: www.ijirset.com

Vol. 6, Issue 4, April 2017

phase angles of the voltage at the k^{th} and m^{th} buses, and $|Y_{km}|, \theta_{km}$ are the bus admittance magnitude and its angle between the k^{th} and m^{th} buses.

5.2.2 Inequality constraints:

These are the constraints represents the system operational and security limits which are continuous and discrete constraints.

Generator bus voltage limits:

$$V_{G_i}^{min} \leq V_{G_i} \leq V_{G_i}^{max} \quad \forall i \in NG$$

Active power generation limits:

$$P_{G_i}^{min} \leq P_{G_i} \leq P_{G_i}^{max} \quad \forall i \in NG$$

Transformers tap setting limits:

$$T_i^{min} \leq T_i \leq T_i^{max} \quad \forall i \in nt$$

Capacitor reactive power generation limits:

$$Q_{sh_i}^{min} \leq Q_{sh_i} \leq Q_{sh_i}^{max} \quad \forall i \in nc$$

Transmission line flow limit:

$$S_{l_i} \leq S_{l_i}^{max} \quad \forall i \in nl$$

Reactive power generation limits:

$$Q_{G_i}^{min} \leq Q_{G_i} \leq Q_{G_i}^{max} \quad \forall i \in NG$$

Load bus voltage magnitude limits:

$$V_i^{min} \leq V_i \leq V_i^{max} \quad \forall i \in NL$$

The control variables in this problem are self-constrained, whereas the in-equality constraints such as P_{G_i}, V_i, Q_{G_i} , and S_{l_i} are non-self-constrained by nature. Hence, these inequalities are incorporated into the objective function using a penalty approach [18]. The augmented function can be formulated as:

$$A_{aug}(x, u) = A(x, u) + R_1 (P_{G_1} - P_{G_1}^{lim})^2 + R_2 \sum_{i=1}^{NL} (V_i - V_i^{lim})^2 + R_3 \sum_{i=1}^{NG} (Q_{G_i} - Q_{G_i}^{lim})^2 + R_4 \sum_{i=1}^{nl} (S_{l_i} - S_{l_i}^{max})^2 \quad (33)$$

where R_1, R_2, R_3 , and R_4 are the penalty quotients, which take large positive values. The limit values of the dependent variable x^{lim} can be given as:

$$x^{lim} = \begin{cases} x, & x^{min} \leq x \leq x^{max} \\ x^{max}, & x \geq x^{max} \\ x^{min}, & x \leq x^{min} \end{cases}$$

Where, ' x^{lim} ', can be P_{G_1}, V_i, Q_{G_i} .

VI. GRAVITATIONAL SEARCH ALGORITHM

The GSA could be considered as an isolated system of masses. It is like a small artificial world of masses obeying the Newtonian laws of gravitation and motion. More precisely, masses obey the following laws:

The gravitational constant, G, is initialized at the beginning and will be reduced with time to control the search accuracy. In other words, G is a function of the initial value (G_0) and time (t):

$$G(t) = G(0) \times \exp\left(\frac{-\alpha t_i}{T}\right) \quad (34)$$

Where, α is a constant, t_i is the iteration number and 'T' is the total number of iterations.

Consider a system of N agents. The position of i^{th} agent is defined as

International Journal of Innovative Research in Science, Engineering and Technology

(An ISO 3297: 2007 Certified Organization)

Website: www.ijirset.com

Vol. 6, Issue 4, April 2017

$$X_i = (x_i^1, \dots, x_i^d, \dots, x_i^n) \quad ; \quad i = 1, 2, 3, \dots, N \quad (35)$$

For each position fitness function is evaluated.

6.1. Calculation of masses

Let $fit_i(t)$ be the fitness function of i^{th} particle at t^{th} iteration.

Now we introduce new variables $worst(t)$ and $best(t)$.

For a minimization problem, $worst(t)$ and $best(t)$ are defined as follows:

$$best(t) = \min(fit_j(t)) \quad ; \quad j = 1, 2, \dots, N \quad (36a)$$

$$worst(t) = \max(fit_j(t)) \quad ; \quad j = 1, 2, \dots, N \quad (36b)$$

For a maximization problem, $worst(t)$ and $best(t)$ are defined as follows:

$$best(t) = \max(fit_j(t)) \quad ; \quad j = 1, 2, \dots, N \quad (37a)$$

$$worst(t) = \min(fit_j(t)) \quad ; \quad j = 1, 2, \dots, N \quad (37b)$$

Gravitational and inertia masses are simply calculated by the fitness evaluation. A heavier mass means a more efficient agent. This means that better agents have higher attractions and walk more slowly. Assuming the equality of the gravitational and inertia mass, the values of masses are calculated using the map of fitness. We update the gravitational and inertial masses by the following equations:

$$M_{ai} = M_{pi} = M_{ii} = M_i \quad (38a) \quad m_i(t) = \frac{fit_i(t) - worst(t)}{best(t) - worst(t)} \quad (38b) \quad M_i(t) = \frac{m_i(t)}{\sum_{j=1}^N m_i(t)}$$

(38c)

6.2. Calculation of force

For iteration t , we define the force acting on mass i from mass j as following

$$F_{ij}^d(t) = G(t) \frac{M_{pi}(t)M_{aj}(t)}{R_{ij} + \epsilon} (x_j^d - x_i^d) \quad (39)$$

Where, M_{ai} , M_{pi} are the active and passive gravitational masses related to agent j , $G(t)$ is gravitational constant at iteration t , ϵ is a small constant and R_{ij} is the Euclidian distance between two agents i and j given by

$$R_{ij}(t) = \|X_i(t) - X_j(t)\|_2 \quad (40)$$

Since M is a function of m , which is function fitness, in every iteration, one value of m is zero. Hence M is zero at this value of m . At this value of M acceleration becomes an indefinite value from above equations. To obtain integer value of K_{best} , it is rounded in terms of population. Hence we introduce another variable E which is defined as follows:

$$E_{ij}^d = \frac{F_{ij}^d}{MG} = \frac{M}{R_{ij} + \epsilon} (x_j^d - x_i^d) \quad (41) \quad E_i^d(t) = \sum_{j=1, j \neq i}^N rand_i E_{ij}^d(t) \quad (42)$$

6.3. Calculation of acceleration

Hence, by the law of motion, the acceleration of the agent ' i ' at iteration t , and in direction d , is given as:

$$a_i^d = E_i^d(t) \times G(t) \quad (43)$$

Furthermore, the next velocity of an agent is considered as a fraction of its current velocity added to its acceleration. Therefore, its position and its velocity could be calculated as follows:

$$V_i^d(t+1) = rand_i \times V_i^d(t) + a_i^d(t) \quad (44a) \quad x_i^d(t+1) = x_i^d(t) + V_i^d(t+1) \quad (44b)$$

International Journal of Innovative Research in Science, Engineering and Technology

(An ISO 3297: 2007 Certified Organization)

Website: www.ijirset.com

Vol. 6, Issue 4, April 2017

VII. RESULTS AND ANALYSIS

In order to demonstrate the effectiveness and robustness of the proposed GSA method with TCSC, IEEE 30 bus system is considered. The existing and proposed methodologies are implemented on a personal computer with Intel Core2Duo 1.18 GHz processor and 2 GB RAM. The input parameters of the proposed GSA method for the considered test system are given in Table.1.

Table.1 Input parameters for test system

S. No	Optimization Method	Parameters	Quantity
1	GSA method	Population	50
		Maximum iterations	100
		Initial gravitational constant (G_0)	100
		Decay constant (α)	5/10
		Constant (ϵ)	8.854×10^{-12}
		Percentage of number of particles in final iteration	2
		Rnorm	2

This section presents the details of the study carried out on IEEE-30 bus test system to analyze OPF problem. The network and load data for this system is taken from [19]. In the IEEE 30-bus system consist 41 branches, six generator buses and 21 load buses. Four branches 6-9, 6-10, 4-12 and 27-28 have tap changing transformers. The buses with possible reactive power source installations are 10 and 24.

As the SVC is a shunt controlled FACTS device, the bus which suffers from high voltage stability index is required to install SVC. From the VSI values at load buses, it is identified that, bus-30 has the highest VSI value and is suitable to install SVC, because of this the VSI value has been enhanced.

From the base case analysis and from the power flows, it is observed that, the best location to install TCSC is between buses 29 and 30 i.e. line-39. For this line, the actual thermal limits is 16 MVA but at the actual flow is 3.753 MVA, there is a margin of 12.247 MVA for which we can increase the power flow.

From the above analysis, the optimal location to install SVC is bus 30 and for TCSC is line-30 between buses 29 and 30. The further analysis is assumed by placing these devices in these locations.

In this, the results of optimized values for all control variables for maximization of system loadability as objective with proposed GSA method. The summary of test results with TCSC or/and SVC are given in Table 2. The convergence characteristics of the proposed algorithm for all the cases are shown in Fig.5.

From Table.2, it is observed that the loadability is increased by 0.04469 with TCSC, 0.00577 with SVC and 0.0786 with both devices. Similarly, the respective losses with all devices are also tabulated.

Table.2. OPF results of loadability with SVC or/and TCSC for IEEE-30 bus system

S. No	Control parameters	Without device	With			
			TCSC	SVC	TCSC & SVC	
1	Real power Generation (MW)	P_{G1}	191.678	197.1671	189.2307	193.1987
		P_{G2}	75.41408	80	79.98629	80
		P_{G5}	37.14777	48.25995	34.79076	45.36324
		P_{G8}	12.91074	26.79696	24.08849	35

International Journal of Innovative Research in Science, Engineering and Technology

(An ISO 3297: 2007 Certified Organization)

Website: www.ijirset.com

Vol. 6, Issue 4, April 2017

		P_{G11}	29.2394	30	27.23448	23.85008
		P_{G13}	37.67434	16.72953	29.94449	28.26867
2	tapGenerator voltages (p.u.)	V_{G1}	1.045264	0.964434	1.062438	1.065806
		V_{G2}	1.021898	0.95	1.009567	1.037103
		V_{G5}	1.011296	0.952396	1.006513	0.995525
		V_{G8}	0.977802	0.950319	1.006799	1.035644
		V_{G11}	1.073999	1.059449	1.030612	1.040192
		V_{G13}	0.987059	1.090957	1.022277	1.063218
3	Transformer setting (p.u.)	T_{6-9}	1.051769	1.011216	1.013111	0.976109
		T_{6-10}	0.905091	1.070171	1.028202	0.937742
		T_{4-12}	0.96908	1.016251	0.940131	0.9486
		T_{28-27}	0.912164	1.002286	1.034353	0.9
4	Shunt compensators (MVar)	$Q_{C,10}$	12.60878	19.4833	16.57989	21.61214
		$Q_{C,24}$	22.81611	12.71165	21.91046	30
5	X _{tcsc} . P.u.	-	-0.57632	-	0.17373	
6	Q _{svc} , MVar	-	-	0.9383	0.567162	
7	Total generation (MW)	384.0643	398.9536	385.2752	405.6807	
8	Loadability index (LBI)	0.30474	0.34943	0.31051	0.38334	
9	Non-convex fuel cost (\$/h)	1287.433	1352.356	1281.224	1373.97	
10	Emission (ton/h)	0.399909	0.423151	0.394844	0.40682	
11	Total power losses (MW)	14.30102	16.5251	13.87667	13.64209	

From Fig.5, it is observed that, in the presence of both devices, the iterative process starts with good function value and reached final best value in more number of iterations when compared to without and with TCSC and SVC. This is because of solving OPF in the presence of devices.

International Journal of Innovative Research in Science, Engineering and Technology

(An ISO 3297: 2007 Certified Organization)

Website: www.ijirset.com

Vol. 6, Issue 4, April 2017

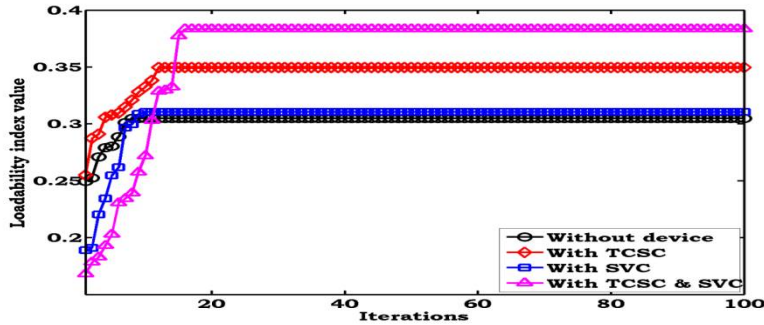


Fig.5. Convergence characteristics of loadability with SVC or/and TCSC for IEEE-30 bus system

The voltage magnitudes in transmission lines with SVC, TCSC, TCSC & SVC devices and without device for IEEE-30 bus system are tabulated in table.3

Table.3 Voltage magnitudes of loadability with SVC or/and TCSC for IEEE-30 bus system

Bus No	Without device	With		
		TCSC	SVC	TCSC & SVC
1	1.065806	1.0624379	1.04526415	0.9644341
2	1.0371031	1.0259712	1.02189751	0.95
3	1.0215899	1.0159032	1.0011717	0.9514227
4	1.0116518	1.0054217	0.99125554	0.9486233
5	0.995525	1.0065125	1.01129639	0.9523965
6	1.0064788	1.0071102	0.98582751	0.9486157
7	0.9905242	0.9961571	0.9854361	0.938224
8	1.0120417	1.0132353	0.97780183	0.9503189
9	1.03876	1.0009681	1.0015992	0.976054
10	1.0439585	0.9910995	0.99938035	0.9549928
11	1.0401925	1.0306123	1.07399941	1.0594493
12	1.0496065	1.0151227	0.9904785	0.9856306
13	1.0632179	1.0222771	0.9870593	1.0643093
14	1.0339256	0.9954818	0.97609725	0.9626258
15	1.031779	0.9891526	0.97484188	0.9548858
16	1.0370083	0.9948541	0.98384704	0.9622399
17	1.0344109	0.9848227	0.98725406	0.9493641

International Journal of Innovative Research in Science, Engineering and Technology

(An ISO 3297: 2007 Certified Organization)

Website: www.ijirset.com

Vol. 6, Issue 4, April 2017

18	1.0190538	0.972923	0.96651893	0.9368524
19	1.0159172	0.9676814	0.96600911	0.9308121
20	1.0218152	0.9724285	0.97322922	0.9356791
21	1.0344779	0.977955	0.98805697	0.9385604
22	1.0376412	0.9799677	0.99055897	0.9399834
23	1.0356218	0.9800543	0.9793448	0.9389953
24	1.0526671	0.9797967	0.9973673	0.9302706
25	1.0593082	0.958361	1.00823237	0.9145222
26	1.035695	0.933535	0.98480811	0.9102923
27	1.0749017	0.9571714	1.02647215	0.9178828
28	1.0002345	1.0049955	0.97596111	0.9437086
29	1.0484085	0.9285942	1.00024231	0.91822
30	1.0330995	0.9120944	0.98508776	0.93272

The variation of voltage magnitude of loadability with SVC, TCSC, TCSC & SVC devices and without device for IEEE-30 bus system are as shown in Fig.6.. With both TCSC and SVC the generators are rescheduled and voltage profile is enhanced when compared to remaining cases.

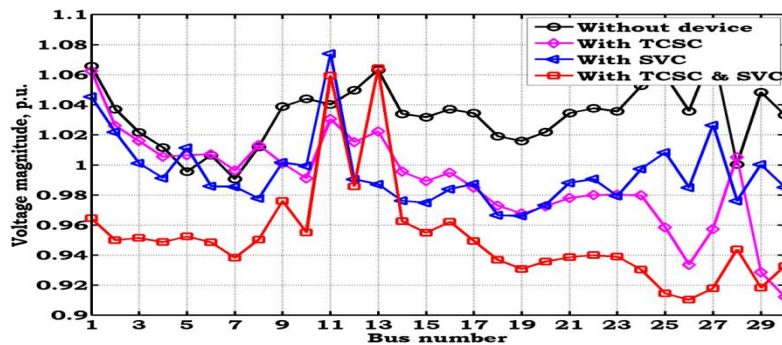


Fig.6. Variation of voltage magnitudes of loadability with SVC or/and TCSC for IEEE-30 bus system

The power flows of loadability with SVC, TCSC, TCSC & SVC devices and without device for IEEE-30 bus system are tabulated in table.4.

International Journal of Innovative Research in Science, Engineering and Technology

(An ISO 3297: 2007 Certified Organization)

Website: www.ijirset.com

Vol. 6, Issue 4, April 2017

Table.4 Power flows of loadability with SVC or/and TCSC for IEEE-30 bus system

Line No	Without device	With			MVA Limit
		TCSC	SVC	TCSC & SVC	
1	127.0507	126.43874	127.82343	126.70404	130
2	65.442723	66.6448	70.608249	67.834902	130
3	39.376495	40.682989	45.665603	41.933454	65
4	59.974214	61.081823	66.283779	62.12295	130
5	78.723197	78.280267	76.002882	76.662904	130
6	54.10937	53.984961	58.030965	55.099475	65
7	64.697389	60.367579	56.360842	58.081975	90
8	27.863159	18.868512	15.438019	13.642033	70
9	42.947309	43.83242	38.525596	43.631692	130
10	29.428716	26.510129	18.571341	20.137703	32
11	31.017725	15.265003	24.574706	19.012001	65
12	22.688743	13.700013	17.997995	17.197327	32
13	44.87102	30.404602	48.593904	23.850669	65
14	40.792325	43.351161	51.999192	42.732974	65
15	26.808181	40.841082	45.054107	34.921727	65
16	37.830707	30.293101	57.68399	29.887654	65
17	10.248964	11.222115	11.374639	10.785083	32
18	24.940821	27.11185	26.619924	25.525241	32
19	11.13619	12.385707	11.460401	10.671996	32
20	2.5491617	2.6379545	2.5498595	2.2597051	16
21	7.67836	7.0038474	6.136663	5.6733054	16
22	8.3941748	9.2933422	8.6258468	8.6880231	16
23	4.4496766	4.7956516	4.2132391	4.0047188	16
24	10.285836	8.4555542	9.8845771	10.097694	32
25	13.603038	11.743008	13.303294	13.619591	32
26	13.415462	7.5086602	8.9802256	11.470365	32
27	21.071044	22.735588	24.933675	21.438651	32

International Journal of Innovative Research in Science, Engineering and Technology

(An ISO 3297: 2007 Certified Organization)

Website: www.ijirset.com

Vol. 6, Issue 4, April 2017

28	9.757447	10.710057	11.873475	10.045018	32
29	9.5311914	7.7015268	5.1898492	12.70043	32
30	9.371814	8.7544684	8.2582876	9.053332	16
31	10.573832	10.195995	9.7406238	14.520568	16
32	8.6027399	4.9288276	3.2963381	8.2794608	16
33	2.8622044	5.6964828	4.1287535	2.9113876	16
34	5.5943263	5.6344774	5.8227501	5.9256251	16
35	8.3378023	3.8363475	4.2650558	8.6820501	16
36	26.970588	21.236961	23.436226	28.71845	65
37	8.4416043	8.5336099	8.8389957	8.9380768	16
38	9.5976144	9.7065166	10.057989	10.161135	16
39	4.9177304	4.9545174	5.1159808	5.2106694	16
40	1.8365256	2.4666961	2.6314295	5.038918	32
41	24.615312	18.883149	19.985256	22.347262	32

The flows of loadability with SVC, TCSC, TCSC & SVC devices and without device for IEEE-30 bus system are as shown in Fig.7. From these figures, 6 & 7 the voltage profile and transmission line loadings are enhanced in the presence of both of the devices instead of single device.

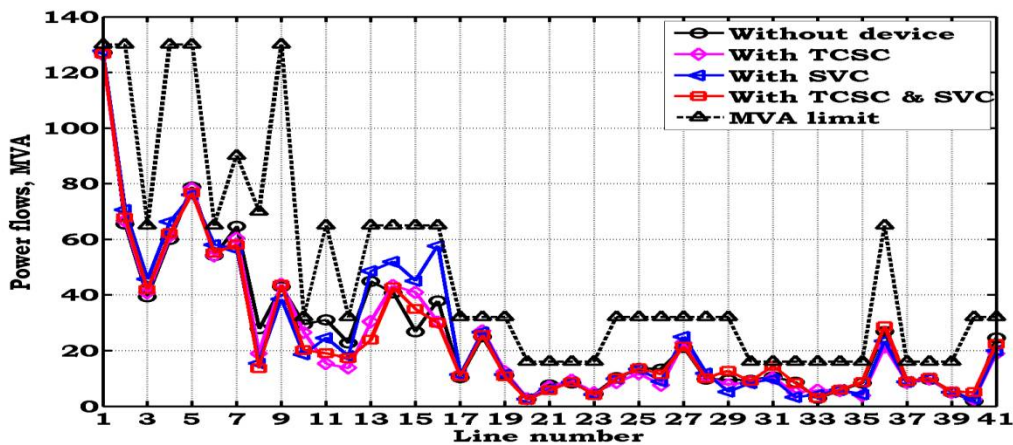


Fig.7. Variation of power flows of loadability with SVC or/and TCSC for IEEE-30 bus system

International Journal of Innovative Research in Science, Engineering and Technology

(An ISO 3297: 2007 Certified Organization)

Website: www.ijirset.com

Vol. 6, Issue 4, April 2017

VIII. CONCLUSION

In this paper, the loadability enhancement problem with loadability objective is solved in the presence of TCSC and SVC while satisfying system, constraints and device limits. The effect of these FACTS controllers on bus voltage magnitudes and line power flows has been analyzed. The OPF results obtained in the presence of both TCSC and SVC are compared with that of the results obtained in the presence of individual controllers. The proposed methodology has been tested on standard IEEE-30 bus test system.

REFERENCES

- [1] M.Gitizadeh and M.Kalantar "A new approach for congestion management via optimal location of FACTS devices in deregulated power systems", Proceedings of DRPT conference, Nanjing, China, 6-9 April 2008.
- [2] Seyed Abbas Taher and Hadi Besharat "Transmission congestion management by determining optimal location of FACTS devices in deregulated power systems", American Journal of Applied Sciences 5(3), pp.24-247, 2008.
- [3] T.K.P. Medicherla, R. Billinton, M. S. Sachadev, "Generation rescheduling and load shedding to alleviate line over loads: analysis", IEEE Trans. on PAS, Vol.98, No.12, pp.1876-1884, 1979.
- [4] T K P Medicherla, R Billinton, and M S Sachadev, "Generation rescheduling and load shedding to alleviate line over loads: system studies", IEEE Transactions on PAS, Vol.100, No.1, pp.36-42, 1981.
- [5] R.J.Ringlee and D.D.Williams, "Economic dispatch operation considering valve throttling losses, II- Distribution of system loads by the method of dynamic programming", IEEE Transactions on Power Apparatus and Systems, Vol.82, No.1, pp.615-620, 1963.
- [6] E.Sortomme, M. A. El-Sharkawi. "Optimal power flow for a system of microgrids with controllable loads and battery storage,"Power systems conference and exposition, PSCE, Seattle, WA, 1-5, Mar., 2009.
- [7] R.J.Ringlee and D.D.William, "Economic dispatch operation considering valve throttling losses. Part II: Distribution of system loads by the method of dynamic programming", IEEE Transactions on Power Apparatus and Systems, Vol.82, No.1, 1963.
- [8] K.Iba l. "Calculation of critical loading condition with nose curve using homotopy continuation method", IEEE Trans. Power Systems, Vol. 6, May 1991, pp. 584-593.
- [9] H.D. Chiang, A. Flueck, K.S. Shah, N. Balu, "CPFLOW: A practical tool for tracing power system steady-state stationary behavior due to load and generation variations", IEEE Trans. Power Systems, vol. 10, no. 2, pp. 623-634, May 1995,.
- [10] S. Greene, I. Dobson, F.L. Alvarado, "Sensitivity of the loading margin to voltage collapse with respect to arbitrary parameters", IEEE Trans. on power systems, Vol. 12, No. 1, pp. 262-272, February 1997.